European Journal of Orthodontics 23 (2001) 517–527

Three-dimensional finite element modelling of a dog skull for the simulation of initial orthopaedic displacements

V. Verrue, L. Dermaut and B. Verhegghe*
Departments of Orthodontics and *Applied Mechanics, University of Gent, Belgium

SUMMARY From 55 frontal tomograms (CT-scans) using the 'Patran' finite element processor, a three-dimensional finite element model (FEM) of a dog skull was constructed. The model was used to calculate bone displacements under orthopaedic loads. This required good representation of the complex anatomy of the skull. Five different entities were distinguished: cortical and cancellous bone, teeth, acrylic and sutures. The first model consisted of 3007 elements and 5323 nodes, including three sutures, and the second model 3579 elements and 6859 nodes, including 18 sutures. Prior to construction of the FEM, an *in vivo* study was undertaken using the same dog. The initial orthopaedic displacements of the maxilla were measured using laser speckle interferometry. Under the same loading conditions, using the second FEM, bone displacements of the maxilla were calculated and the results were compared with the *in vivo* measurements. Compared with the initial displacement measured *in vivo*, the value of the constructed FEM to simulate the orthopaedic effect of extra-oral force application was high for cervical traction and acceptable for anterior traction.

Introduction

The use of orthopaedic appliances has increased steadily over several decades. Extra-oral forces are applied in an attempt to control and change the amount and/or direction of growth of the maxilla. In order to understand the biological and biomechanical response of the maxilla to an applied orthopaedic force system, it is important to investigate the influence of the amount, the direction, the point of application and the duration of the applied traction, as well as the influence of the craniofacial morphology and the age of the patient. Classical growth studies are not able to predict the biological effect of orthopaedic force systems. It remains difficult to distinguish the orthopaedic effect of extra-oral force from normal growth. That is why in the majority of clinical studies an experimental group is compared with an untreated control group. However due to important individual variations in biological parameters (such as growth and morphology) a very large sample is required to allow statistically revelant conclusions to be drawn.

Because of these limitations there has been an increased interest in studies in which extra-oral traction is tested on 'models' (photo-elastic models, macerated dry and wet skulls, finite element models, etc.). Various *in vitro* measuring techniques have been developed to study the effect of orthopaedic force systems. Strain gauges (Nakanishi, 1973; Miura *et al*., 1980; Kannan, 1982; Ichikwa *et al*., 1984; Tanne *et al*., 1985), double exposure holography (Nanda, 1978; Dermaut and Beerden, 1981) and laser speckle interferometry (Kragt, 1979; Dermaut *et al*., 1986; Kragt and Duterloo, 1982, 1983; Kragt *et al*., 1982, 1986; Pavlin and Vukicevic, 1984; Arai, 1985; De Clerck *et al*., 1990; Govaert and Dermaut, 1997) are all highly sensitive techniques able to measure extremely small initial deformations of bone on macerated skulls. Unfortunately, most of these techniques are limited in their ability to measure internal displacements and strain–stress levels in a complicated structure such as the craniofacial skeleton.

On the other hand, the finite element method (FEM), which has been successfully applied to

the mechanical study of stresses and strains in the field of engineering, makes it practicable to elucidate biomechanical components, such as displacements in living structures from various external forces. Moreover it is an appropriate method that can represent the irregular geometry and lack of homogeneity of bone. The most important advantage of this model is the ability to test an unlimited number of force application systems once an adequate FEM is created. Recently the FEM has been a frequently used technique in the field of medical science (Begis *et al*., 1988; Galbraith and Bryant, 1989; Huiskes and Boeklagen, 1989; Schmitt *et al.*, 1995) and dentistry (Cook *et al*., 1982; Tanne *et al*., 1987).

Many studies have used a simple two-dimensional (2D) FEM (Carter *et al*., 1984; Farah *et al.*, 1988; Weinans *et al.*, 1990) which has its limitations in orthopaedic research. Whilst they offer the possibility of high mesh refinement and can predict the inhomogeneity of bone, they cannot represent the three-dimensional (3D) complex structure of bone nor the 3D nature of intrinsic stress patterns. On the other hand, many 3D models are generated from 'average' bone geometry (Rubin *et al*., 1983; Wilson *et al.*, 1991) despite their inability to provide clinically vital, patient-specific estimations.

Tanne *et al.* (1989) and Iseri *et al.* (1998) developed a 3D FEM of the craniofacial skeleton of a particular patient's skull and proposed a model with fine division. They believed that such modelling could lead to more accurate results. However, the study of a 'model' is valid only when a distinct link can be demonstrated between initial bone displacement in the model and the eventual orthopaedic effect on the craniofacial skeleton under identical traction. Primary to this hypothesis is that a relationship or correspondence has to be proven between initial bone displacement *in vivo* and initial bone displacement of the model.

The aim of this study was to create a 3D subject-specific FEM of the craniofacial skeleton in an attempt to test and evaluate the effect of extra-oral force systems on this model. For this investigation, the skull of dog A, described in the *in vivo* study of Govaert and Dermaut (1997), was used. The calculated initial displacement of the FEM of the same animal was compared with the initial bone displacement *in vivo* as reported by Govaert and Dermaut (1997).

Methods

In vivo study

Previous to the creation of the FEM, an *in vivo* study was undertaken (Govaert and Dermaut, 1997) to measure initial bone displacement *in vivo*. In that experiment an 11 month-old female Alsatian dog was used. The dog was selected as the experimental model, because of the strong ventral or anterior development of the maxilla, which is advantageous for registering orthopaedic displacements in this area. The age of the dog was chosen so that it approaches the clinical circumstances of successful orthopaedic treatment, which in the growing child is up to about 13 years. At that stage the sutures of the craniofacial skeleton are still open, or not completely fused.

Initial bone displacements of the maxilla were measured by means of laser speckle interferometry. This sensitive technique makes it possible to measure extremely small displacements. To test the error of the method the apparatus designed by De Clerck *et al*. (1990), which reproduces very small rotations with great accuracy, was used (Figure 1). The displacement vectors were calculated at three measuring points on the rectangular measuring plate (1 on Figure 1) by means of laser speckle interferometry. The location of the centre of

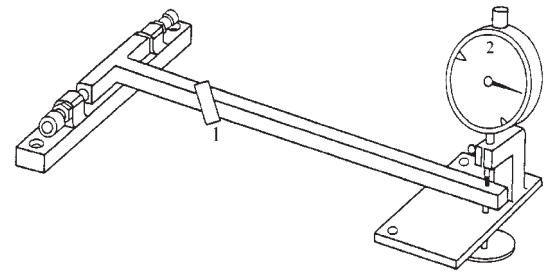

Figure 1 T-device with measuring plate (1) and displacement gauge (2).

rotation was compared with that of the axis rotation. The amount of the displacement, calculated by means of speckle interferometry, was compared with the amount of displacement on the dial gauge. A total of 18 experiments were undertaken. With the equipment used, displacements ranging between 3.5 and 1000 μm could be measured. The location of the centres of rotation and the amount of displacement, calculated with speckle interferometry, proved to be equal to the location of the real axis of rotation and the amount of displacement measured with the dial gauge. For displacements larger than 10 μm measurement errors of approximately 1 degree and 1 μm were found.

The displacements of the maxilla were registered with reference to the frontal bone. Because the measurements were in the range of a few microns, a rigid fixation of the frontal bone was essential. De Clerck *et al.* (1990) introduced and tested a specially designed frontal clamp: four pins were screwed against the skull and four supports were pulled against the orbital roof (Figure 2). The head of the anaesthesized dog with the clamp was fixed onto an L-shaped stand. Two measuring plates were, through a metal wire, fixed, one to the bone surface of the maxilla, and the other to the posterior part of the zygomatic arch to allow control of the stability of the clamp. No displacements were observed at the zygomatic arch, indicating that the fixation of the skull was adequate.

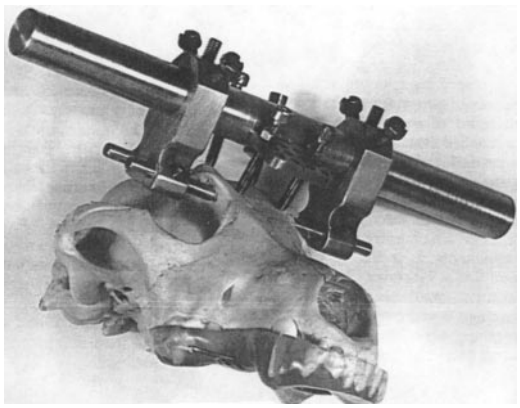

Figure 2 The frontal clamp.

A double exposure optical technique was used. A photographic registration was first undertaken before applying force to the maxilla, and the image of the head of the dog together with a speckle pattern was registered on this photograph. A force application of 8.5 N was exerted on an acrylic splint covering the upper teeth. In the experiments, forces were applied in three different directions: protral, cervical and high-pull. A system consisting of pulleys was designed to standardize the different tractions. Nylon threads ran from the metal bar in the acrylic dental splint (point of force application) over various pulleys to a bar with several weights, which influenced the amount of force on the dental splint and therefore on the maxilla. The in-between position of various pulleys allowed for protral, cervical and high-pull traction. To define the exact direction of the three different force vectors, a line through the point of force application (in the sagittal plane) was drawn parallel to the line connecting the posterior orbital fixation point with the posterior border of the acrylic splint (Figure 3). The line was used as reference to define protral (146 degrees), cervical (112 degrees) and high-pull traction (10 degrees). After loading, a second photograph on top of the first one was taken on the same film which permitted registration of the speckle pattern by the double exposure procedure. By directing laser light through the developed film a fringe pattern was created. The direction and the number of fringes indicated the direction and magnitude of the displacement which was defined by displacement vectors.

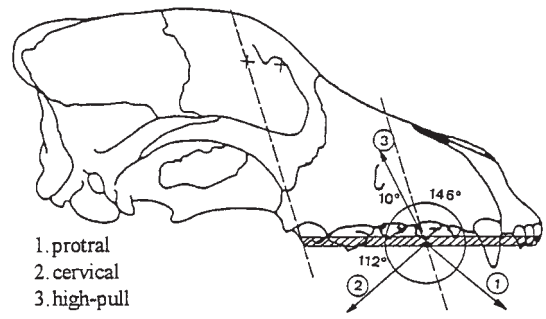

Figure 3 The three directions of traction applied to the splint.

In this *in vivo* study no reliable displacement caused by high-pull traction could be measured. It can be assumed that by using high-pull forces the sutures are compressed to some extent and therefore initial displacements are difficult to measure. This is in agreement with the findings of Kragt (1979), Kragt and Duterloo (1982, 1983) and Kragt *et al*. (1982, 1986).

Finite element simulation

Finite element analysis (FEA) is a numerical method that is able to calculate, under specific loads and boundary conditions, displacements, stresses and strains of an arbitrary geometry. Most of the existing programmes can easily generate the geometry of technical parts and structures. The greatest difficulty in this study was the complex geometry of the craniofacial skeleton of the dog, not only because of the irregular form and different component materials, but because of the presence of sutures, which are bone-seams, dividing the skull more or less into different bony parts. From the skull of the dog, used in the *in vivo* study, a FEM was constructed.

In the first part of the study, the skull of the dog was sliced by means of a saw, as described by Tanne *et al*. (1989). The intention was to construct a model starting from a 2D image into a 3D entity. In a first investigation slices of the skull were made by means of a band and a circular saw. A great disadvantage of this technique was the loss of bone material due to the thickness of the saw and the slices breaking into different parts. To overcome this the skull was surrounded, first by plaster, and then by foam. However, the covering material could not reach the internal parts of the skull, resulting in the same problem. In view of this difficulty, tomograms were used to construct the FEM. The radiographic cuts were made by a Siemens CT plus scanner (NV/SA Siemens, Forschein, Germany), with a resolution of 1 mm. Fifty-five frontal tomograms were taken (Figure 4a); 45 of them succeeding each other every 0.5 cm, going from the muzzle to the rear of the skull. The other 10 were taken through specific points of interest: the points of force application, the fixation points of the skull and specific areas of bone displacements. A Hasselblad PCP80, 6×6 projector (V. Hasselbad AB, Goteborg, Sweden) enlarged and projected the tomograms perpendicular to the A2 tracing paper. Standardized magnifications were needed to appropriately construct the model. Hand-made tracings of the tomograms were drawn. Five different materials were distinguished: cortical bone, cancellous bone, teeth, acrylic and sutures. The open sutures consisted of flat, more or less parallel sides. The saw-shaped or interdigitating sutures which

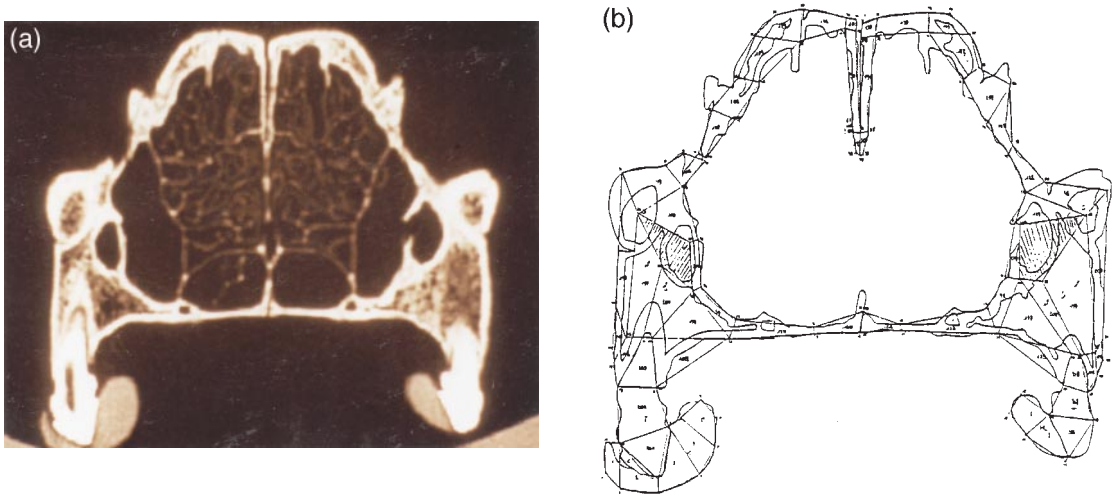

Figure 4 (a) A specific tomogram through the muzzle of the dog skull. (b) The corresponding division in elements of the tomogram of (a).

are complex were almost invisible on the tomographs.

Slice by slice the 2D tracings were divided into elements (Figure 4b). The different materials, contour of the skull, bone thickness, holes in the skull, open sutures, teeth and acrylic splint determined the number of elements, and the refinement of division. The corresponding elements received the same number in all of the slices (taking into account the continuous character of the division of elements of the succeeding slices, and to automate as much as possible the construction of the 3D model).

Because of the complex anatomy of the skull, there was a need to create new elements or skip elements in every slice.

Two-dimensional divisions were digitized and stored on a personal computer. First the locations of the nodes of the elements were digitized and the elements were then defined by determining the approximate centre of gravity of each element. Subsequently the program selected and associated, from the list of nodes, those three (or four) correct nodes belonging to the element. Simultaneously, by highlighting the element, the material of the element was specified and the assembling procedure was checked.

The construction of the 3D model was carried out with the pre-/post-processing program 'Patran' (McNeil Schwendler Corporation, Gouda, The Netherlands, V2.5 and V3). Adjacent cells from two neighbouring sections were connected to form 3D volumes with tetrahedron, wedge or hexagonal forms. Each volume cell was then transformed into one finite element. The elements were first order solid element of the displacement type. The distortion of the elements was checked with the internal test routines of Patran. When the postulated criteria were exceeded, some nodes were moved.

The model was completed by introducing the boundary conditions. The fixation consisted of imposing a zero-displacement and a zero-rotation to the eight fixation points (Figure 5). The loads, the magnitude and the direction of force were introduced at the bottom of the acrylic splint (Figure 2), identical to the *in vivo* study, at the side-points where the metal bar left the splint. At this stage of the study each

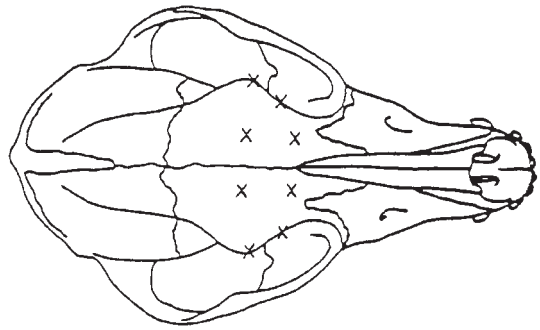

Figure 5 The location of the eight fixation points simulating the fixation.

material number received its corresponding mechanical property, through the elastic modulus or Young's modulus and Poisson's ratio (Table 1). These data were replicated from earlier experiments (Cook *et al.*, 1982) on dog material.

Two models were tested: one in which only open sutures were incorporated (model 1) and the other one in which open as well as interdigitating sutures (model 2) were included.

As the interdigitating sutures were not visible on the tomograms, radio-opaque fluid was used to mark the sutures and new tomograms identical to those of model 1 were taken. With an enlargement projector, the images of the new tomograms were projected and superimposed on the 2D tracings of model 1. Fifteen new sutures were introduced as lines in the tomographic sections. The sutures were modelled with one element over the thickness. An orthotropic material with local axes aligned with the sutures was used. This allowed for different stiffness values along and across the sutures. This is only adapted as a first approximation.

The boundary conditions of model 2 were introduced, analogous to model 1. Only the

Table 1 Elastic properties.[a]

Cortical bone	E = 13,700 N/mm^2, Poisson = 0.3
Cancellous bone	E = 689 N/mm^2, Poisson = 0.3
Teeth	E = 20,700 N/mm^2, Poisson = 0.3
Acrylic	E = 2000 N/mm^2, Poisson = 0.3

[a]Source: Cook *et al.* (1982).

material property of the sutures had to be added. Because no direct data were available, two values of stiffness were introduced, firstly that of the suture was considered as half of the stiffness of cortical bone (E = 6850 N/mm^2) and secondly the stiffness was reduced to a minimum of E = 1 N/mm^2. Due to the 'initial' character of force application and because no changes in time under force load of the apparent Young's modulus occurred, it was not necessary to take visco-elasticity into consideration.

The calculations were carried out with the FEA module of Patran.

Results

Model 1 consisted of 3007 elements and resulted in 5323 nodes. By exerting identical amounts of force to the FEM, the calculated initial bone displacements were only 2–3 μm, despite the open sutures. In the *in vivo* study of Govaert and Dermaut (1997), the amount of displacement was found to be approximately 10 μm. Therefore a second model was constructed in which more sutures were included in an attempt to obtain adequate simulation of the amount of displacement of the *in vivo* situation. Model 2 (Figure 6) consisted of 3579 elements and 6859 nodes.

Introducing the mechanical property E = 6850 N/mm^2 (half of the stiffness of cortical bone) for all the sutures, the displacements were found to be not more than 1 μm.

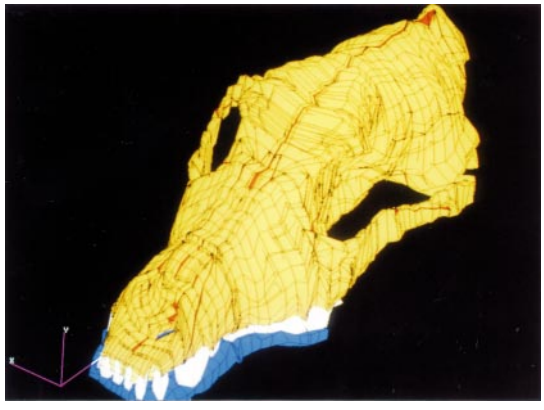

Figure 6 The three-dimensional finite element model of the dog skull.

With a very low E value, E = 1 N/mm^2, the initial bone displacements for the three tractions varied between 6 and 11 μm, which is closer to the values measured *in vivo*.

The calculated displacements of the dentition, connected by an acrylic splint, were not different from the bone displacements, indicating that the applied forces were transferred to the bony part of the skull.

Figures 7, 8 and 9 show the displacement of the anterior part of the skull resulting from cervical traction (Figure 7), anterior or ventral traction (Figure 8) and high-pull traction (Figure 9). It is obvious that the anterior part of the skull rotates ventrally from the nasofrontal suture in a downward or upward direction depending upon the applied force system. The fixation of the posterior and the top part of the skull was adequate, since only very minor displacement was noted in that area. The zygomatic arch was involved to a minor degree in the maxillary movement for the three loading conditions.

Although an attempt was made to build a precise anatomical model by means of FEA, the anterior part of the snout seemed to move as one unit despite the introduction of so many elements. This finding also holds true for the amount of force application (8.5 N) used in this study.

In the FEM the cervical traction resulted in a downward and posterior rotation of the maxilla (Figure 7). Comparing these findings to the displacement vector described by Govaert and Dermaut (1997), there was considerable agreement between both measurements. The direction of displacement of a central point in the maxilla *in vivo* (Govaert and Dermaut, 1997) coincided to an important extent with the displacement of the maxilla in the FEM.

As far as the anterior traction is concerned (Figure 8), a more vertical translation downward was noticed in the FEM. There was less coincidence with the displacement vector found *in vivo*, although a comparable trend could be noticed.

The simulation of the high-pull traction on the FEM (Figure 9) showed an upward and, to some extent, a ventral movement of the maxilla. Since the initial displacement *in vivo* after high-pull

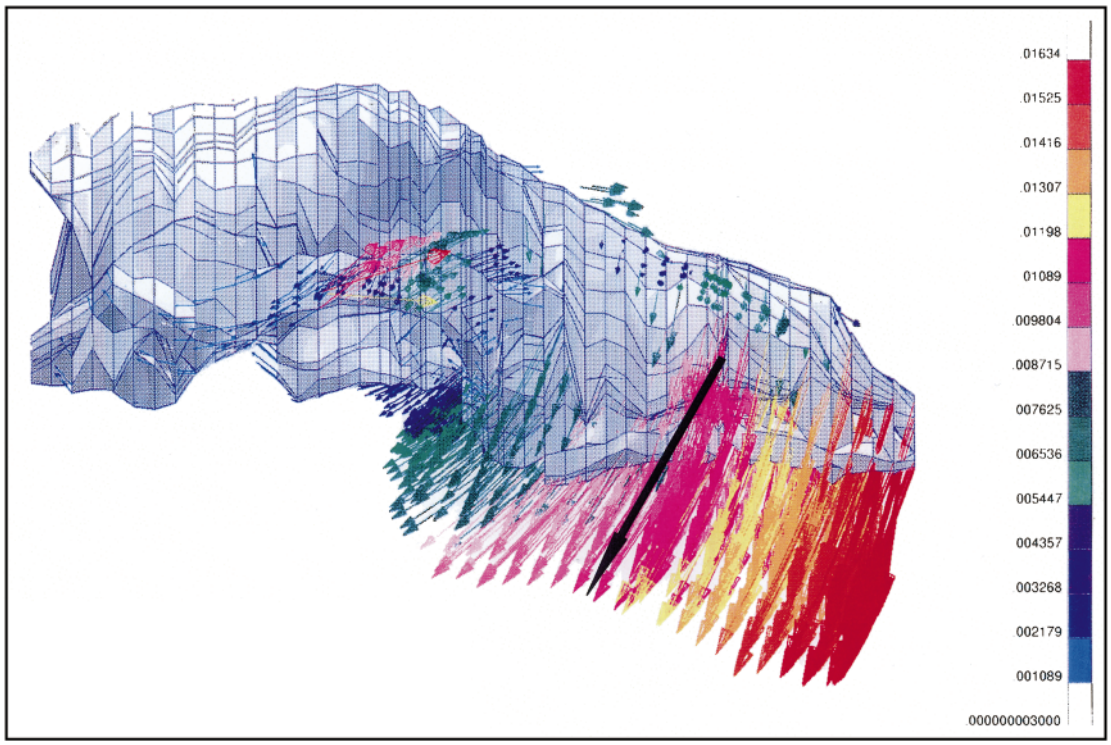

Figure 7 The total deformation of the skull, by means of displacement vectors, after cervical loading, with the superimposed displacement vector (black arrow) measured in the *in vivo* study of Govaert and Dermaut (1997). The colour scale in the figure gives the amplitude of the displacements in millimetres.

traction could not be registered, a comparison with FEM results was not possible.

Discussion

In this study an attempt was made to build a FEM of a dog's skull to simulate the anatomical features as closely as possible. Such a model would enable the study of the effects of force application exerted by orthodontic appliances and to test the effects of orthopaedic extra-oral traction.

Since the skull is a complex structure in which sutures and defects affect the mechanical resistance to force application, the creation of a FEM is a time-consuming procedure. It was found that the localization of the sutures was not easily defineable and manual adaptations were needed to make the model suitable for comparison with the bony skull.

To build an adequate 3D FEM two models were constructed using CT-scans. The second model which was finally used was created due to the limitations of the first. To approach the *in vivo* amounts of displacements, the elastic property of the sutures had to be reduced to the minimum E = 1 N/mm^2. By doing so, the calculated displacements created by headgear and anterior traction could be compared with the initial displacement, measured *in vivo*.

It is obvious that within the craniofacial skeleton, the morphology and location of the sutures play an important and directing role when skeletal displacement is involved. Skeletal age also affects the amount of initial displacement. The dog skull used in this research was 11 months-old and had a maturation comparable with a human skull of approximately 10–13 years of age, used in a number of studies investigating skeletal displacements (Kragt and

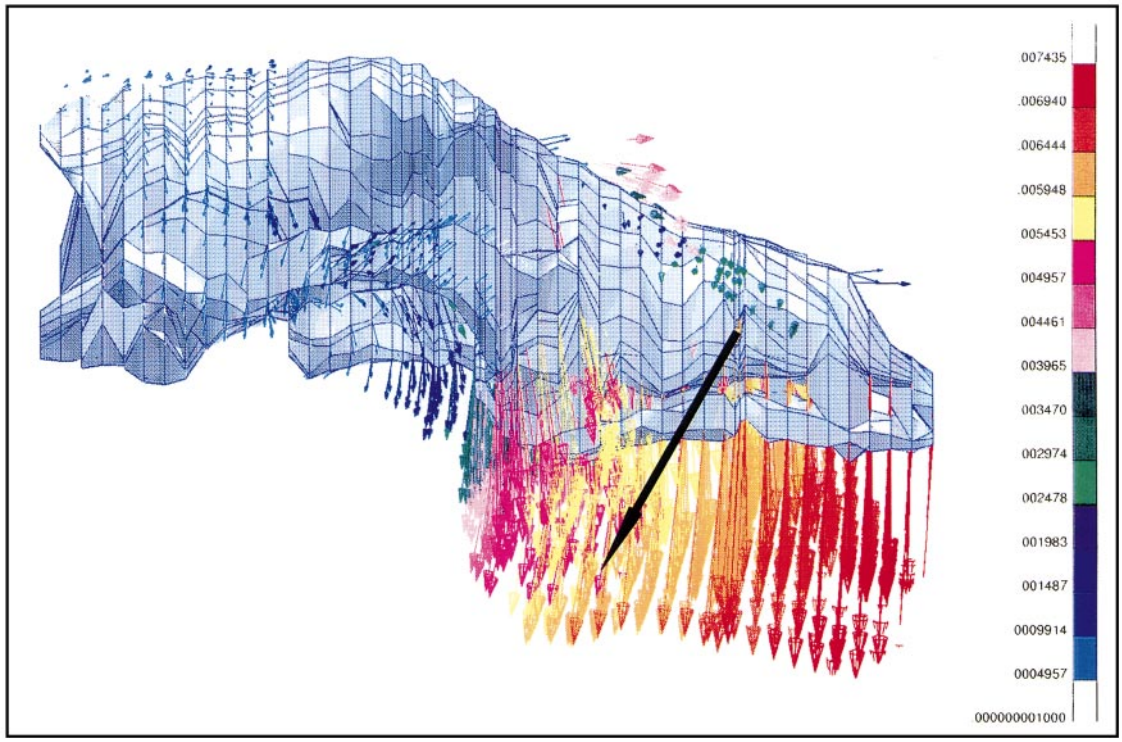

Figure 8 The total deformation of the skull, by means of displacement vectors, after protral loading, with the superimposed displacement vector (black arrow) measured in the *in vivo* study of Govaert and Dermaut (1997).

Duterloo, 1982; Kragt *et al.*, 1986; Tanne *et al.*, 1989).

By studying the displacements measured on the FEM, it was found that the maxilla of the dog seems to move as one unit after different force applications. Bone bending (internal bone deformations) was not noticeable and was negligible compared with the displacement in the sutures. Therefore it might be concluded that the mesh refinement in the craniofacial complex is inferior to the introduction of sutures (localization and properties) in the creation of the model. This finding is at first sight in contradiction with the suggestions made by Tanne *et al.* (1989) that a finer division leads to a more accurate result. In the present experimental set-up, however, the sutures played the most important role for the displacement of the anterior part of the skull.

In the study of Iseri *et al.* (1998), a 3D FEM was constructed based on CT-scans of a human skull of a 12 year-old boy, to investigate bone displacement after 5 mm of palatal expansion. Whilst there was a large similarity in the construction of the 3D structure, instead of directly defining the elements (geometric surfaces) in the 2D slices, through the digitized nodes (geometric points) as in this study, they generated the geometric surfaces from geometric lines, the latter constructed by connecting geometric points.

The FEM in the study of Iseri *et al.* (1998) consisted of 2349 elements and 2147 nodes, and that of model 2 of the dog skull in this investigation of 3579 elements and 6859 nodes. An important difference between the studies is the ratio: quantity of elements/quantity of nodes. In their human FEM study no explanation was given for the integration of the sutures in the model; all sutures were assumed to have the same mechanical properties as the surrounding bone, except at the palatinal bone where it was assumed to be unconnected. Nevertheless,

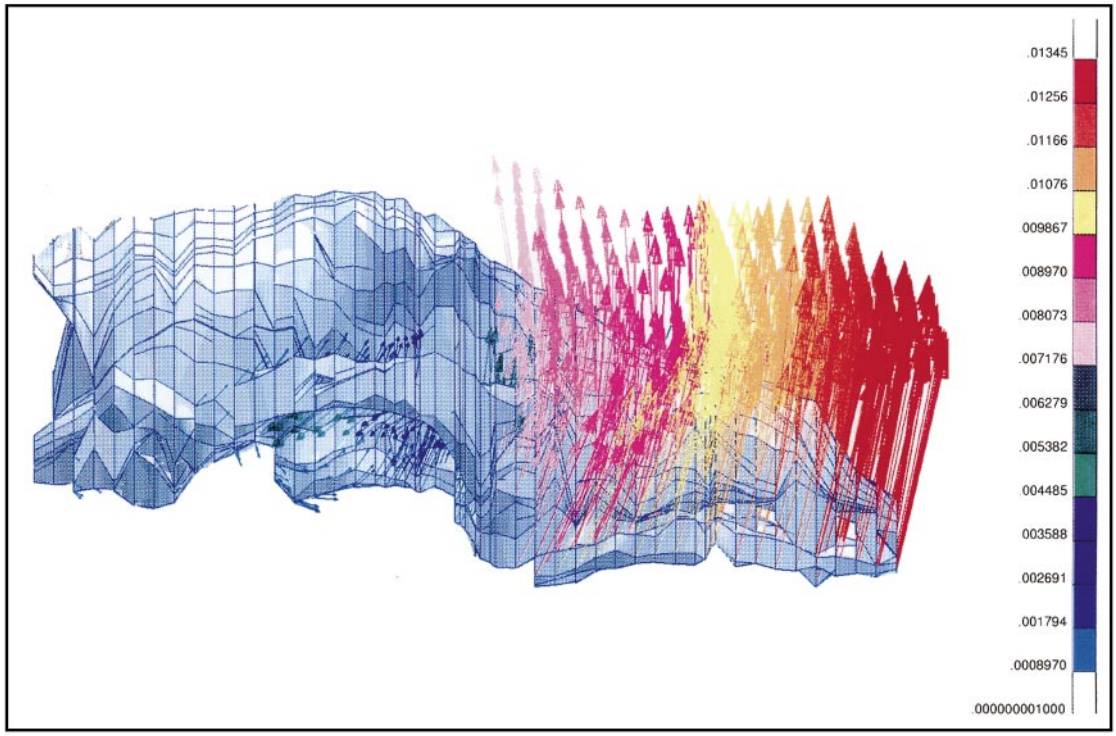

Figure 9 The total deformation of the skull, by means of displacement vectors, after high-pull loading.

without using specific values for the mechanical properties of the sutures, those authors did not incorporate viscoelastic properties. They concluded that future investigations will aim to model the suture as viscoelastic material with hardening properties and experimental studies will be necessary to determine the material properties of sutural structures under growing conditions. In the present study as explained above, an 'initial' force was applied and therefore the viscoelastic character of the sutures was not found to be appropriate.

The present study only attempted to compare the initial *in vivo* displacement to the initial calculated displacement of the FEM. This approach was never followed in earlier studies.

In all traction directions, the anterior part of the skull, located ventrally from the naso-frontal suture, rotated in a downward or upward direction depending upon the applied force system. The posterior aspect part of the skull was not involved in this movement, indicating that fixation of this part of the skull was adequate.

The cervical traction in the FEM resulted in a downward and posterior rotation of the maxilla. Compared with the observed displacement reported in the *in vivo* study of Govaert and Dermaut (1997), a comparable displacement in the FEM was found (Figure 7). Comparison with clinical investigations is difficult, since differences in the anatomy of the skull are obvious. Moreover clinical studies report the longitudinal effects of applied force systems in terms of treatment time. The observed changes are a contribution of normal growth and therapy. In this FEM study, however, only initial displacements were measured.

Kragt *et al.* (1982) found that cervical traction on a macerated human skull resulted in a downward and backward rotation of the maxilla, which is in agreement with the present results. However, they reported that the zygomatic bones

were more affected by the force application than found in this study. Comparison of the study of Kragt *et al.* (1982) and the present investigation is dangerous since their study was carried out on a human skull, which of course has a totally different morphology than the dog skull.

Generally, the high-pull traction in the FEM (Figure 9) produced maxillary displacements in an upward direction but an evaluation of the FEM model could not be carried out as no initial displacements under high-pull loading could be registered *in vivo*. In the study of Kragt and Duterloo (1982) on a macerated skull the maxilla was predominantly displaced in a backward direction. However, the direction of force was 40 degrees upward to the occlusal plane and was applied in the molar region. In the present study on a dog skull, the direction of force was 65 degrees upward to the occlusal plane and was applied in the premolar region. In long-term animal experiments on monkeys (Elder and Tuenge, 1974; Meldrum, 1975) a backward and upward displacement of the maxilla was also reported. Again the morphology of the dog skull is totally different from primate skulls. Comparison between the findings therefore have important limitations.

As far as anterior traction is concerned (Figure 8), an almost vertical translation downward was found in the FEM and the *in vivo* displacement showed a downward and a slightly backward movement of the maxilla.

At least the displacement of the FEM is facing in the same direction as in the *in vivo* situation. In the study of Tanne *et al.* (1989) the horizontal anteriorly directed force on a FEM of a macerated human caused an upward and forward rotation of the nasomaxillary complex, whereas the 30 degrees downward direction to the occlusal plane caused almost a translation of the complex in an anterior direction. The fact that in this investigation a FEM of a dog's skull was used and the direction of force was 40 degrees downward to the occlusal plane could explain the more downward displacement of the maxilla. The most important conclusion, however, remains that the initial *in vivo* displacement of the dog's skull after anterior traction (Govaert and Dermaut, 1997) was comparable with the calculated FEM displacement (Figure 8).

Conclusions

In the present investigation, calculated displacements of a 3D FEM were compared with the 2D changes reported in the *in vivo* study of Govaert (1997).

The 3D FEM provides information to simulate all types of orthodontic force systems and the resulting displacements in three dimensions. Moreover stress and strain can be calculated. These advantages may lead to a more extended analysis of displacements in future research.

To diminish the amount of manual labour, an automated FEM (cf. voxel method) could at first sight be more appropriate, but the introduction of a complicated sutural pattern in the craniofacial skeleton remains a dilemma in finite element modelling.

The value of the 3D FEM to simulate the initial orthopedic effect of extra-oral force application is high for cervical headgear traction and acceptable for protral traction.

The results of this study show that the creation of a FEM of the craniofacial complex automates the 3D division in elements in combination with an accurate and more precise integration of sutures and sutural elastic properties to obtain an improved model.

Address for correspondence

Professor L. Dermaut
University of Gent
Department of Orthodontics
De Pintelaan 185
9000 Gent, Belgium

References

Arai H 1985 A study on the action pattern of maxillary extraoral appliance by means of holography interference method. Journal of the Japanese Orthodontic Society 44: 228–301

Begis D, Delpueck C, Le Tallec P, Loth L, Thiriet M, Vidrascu M 1988 A finite element model of tracheal collapse. Journal of Applied Physiology 64: 1359–1368

Carter D R, Vasu R, Harris W H 1984 Stress changes in the femoral head due to porous ingrowth surface replacement arthroplasty. Journal of Biomechanics 17: 737–747

Cook S D, Weinstein A H, Klawitter J J 1982 A three-dimentional finite element analysis of a porous rooted Co–Cr–Mo alloy dental implant. Journal of Dental Research 61: 25–29

De Clerck H, Dermaut L R, Timmerman H 1990 The value of the macerated skull as a model used in orthopaedic research. European Journal of Orthodontics 12: 263–271

Dermaut L R, Beerden L 1981 The effects of Class II elastic force on a dry skull measured by holographic interferometry. American Journal of Orthodontics 79: 296–304

Dermaut L R, Kleutghen J, De Clerck H 1986 Experimental determination of the center of resistance of the upper first molar in a macerated dry human skull submitted to horizontal headgear traction. American Journal of Orthodontics and Dentofacial Orthopedics 90: 29–36

Elder J R, Tuenge R H 1974 Cephalometric and histologic changes produced by extraoral high-pull traction to the maxilla in *Maccaca mulatta*. American Journal of Orthodontics 66: 599–617

Farah J W, Craig G, Meroueh A 1988 Finite element analysis of a mandibular model. Journal of Oral Rehabilitation 15: 615–624

Galbraith P C, Bryant J T 1989 Effects of grid dimensions on finite element models of an articular surface. Journal of Biomechanics 22: 385–393

Govaert L, Dermaut L R 1997 The importance of humidity in the *in vitro* study of the cranium with regard to initial bone displacement after force application. European Journal of Orthodontics 19: 423–430

Huiskes R, Boeklagen R 1989 Mathematical shape optimization of hip prosthesis design. Journal of Biomechanics 22: 743–804

Ichikawa K, Nakagawa M, Kagomashira K, Hata S, Itoh T, Matsumoto M 1984 The effects of orthopaedic forces on the craniofacial complex utilizing maxillary protraction. Journal of the Japanese Orthodontic Society 43: 325–336

Iseri H, Tekkaya A E, Öztan Ö, Bilgiç S 1998 Biomechanical effects of rapid maxillary expansion on the craniofacial skeleton, studied by the finite element method. European Journal of Orthodontics 20: 347–356

Kannan K 1982 Effects of headgear traction on the facial skeleton of the monkey, a study with strain gauges. Journal of Osaka Dental University 16: 112–136

Kragt G 1979 Measurement of bone displacement in a macerated human skull induced by orthodontic force; a holographic study. Journal of Biomechanics 12: 905–910

Kragt G, Duterloo H S 1982 The initial effects of orthopedic forces: a study of alterations in the craniofacial complex of a macerated human skull owing to high-pull headgear traction. American Journal of Orthodontics 81: 57–64

Kragt G, Duterloo H S 1983 The initial alterations in the craniofacial complex of *Macaca mulatta* skull resulting from forces with high-pull headgear. Journal of Dental Research 62: 388–394

Kragt G, Duterloo H S, ten Bosch J J 1982 The initial reaction of a macerated human skull caused by orthodontic cervical traction determined by laser metrology. American Journal of Orthodontics 81: 49–56

Kragt G, Duterloo H S, Algra A M 1986 Initial displacements and variations of eight human child skulls owing to high-pull headgear traction determined with laser holography. American Journal of Orthodontics 89: 399–406

Meldrum R J 1975 Alterations in upper facial growth of *Macaca mulatta* resulting from high-pull headgear. American Journal of Orthodontics 67: 393–411

Miura H, Nakano H, Yagi M, Kamegai T, Ishikawa F 1980 The experimental study of effects of the upper jaw forward traction on the craniofacial skeleton. Journal of the Japanese Orthodontic Society 39: 229–238

Nakanishi Y 1973 Effects of headgear traction on the human facial skeleton: a study with strain gauges. Journal of Osaka Dental University 7: 7–30

Nanda R 1978 Protraction of maxilla in rhesus monkeys by controlled extraoral forces. American Journal of Orthodontics 74: 121–141

Pavlin D, Vukicevic D 1984 Mechanical reactions of facial skeleton to maxillary expansion determined by laser holography. American Journal of Orthodontics 85: 498–507

Rubin C, Krishnamurthy N, Capilouto E, Yi H 1983 Stress analysis of the human tooth using a three-dimensional finite element model. Journal of Dental Research 62: 82–86

Schmitt J, Leugsfeld M, Alter P, Leppek R 1995 The use of voxel-oriented femur models in stress analysis-preprocessing, calculation and validation of CT-based finite element models. Biomedical Technik 40: 175–181

Tanne K, Miyasaka J, Yamagata Y, Sakuda M, Burstone C J 1985 Biomechanical changes in the craniofacial skeleton by the rapid expansion appliance. Journal of Osaka Dental Society 30: 345–356

Tanne K, Sakuda M, Burstone C J 1987 Three-dimentional finite element analysis for stress in the periodontal tissue by orthodontic forces. American Journal of Orthodontics and Dentofacial Orthopedics 92: 499–505

Tanne K, Hiraga J, Kakiuchi K, Yamagata Y, Sakuda M 1989 Biomechanical effect of anteriorly directed extraoral forces on the craniofacial complex: a study using the finite element method. American Journal of Orthodontics and Dentofacial Orthopedics 95: 200–207

Weinans H, Huiskes R, Grootenboer H J 1990 Trends of mechanical consequences and modeling of a fibrous membrane around femoral hip prostheses. Journal of Biomechanics 23: 991–1000

Wilson A N, Middleton J, McGuinness N, Jones M 1991 A finite element study of canine retraction with a palatal spring. Brittish Journal of Orthodontics 18: 211–218